

On the formation of energy spectra of synchrotron X-rays and inverse Compton γ -rays in binary systems with luminous optical stars

D. Khangulyan* and F. Aharonian*

*MPI für Kernphysik, 69117 Heidelberg, Germany

Abstract. In this paper we study formation broad band energy spectra of electrons due to synchrotron radiation and inverse Compton (IC) scattering. The effect of transition of IC cooling from the Thomson regime to the Klein-Nishina regime can be very significant in the environments where radiation density dominates over the magnetic field density. We discuss impact of this effect on the formation of synchrotron and IC radiation components of TeV electrons in binary systems with very luminous optical stars. Such a scenario can be realized, for example, at the wind termination shock of the pulsar in PSR B1259-63/SS2883 or in the jets of microquasars. The calculations are based on the solution of Boltzmann equation using precise differential Compton cross-section ($d\sigma/d\Omega dE$).

INTRODUCTION

In astrophysical objects where electrons are accelerated to very high energies at the presence of intense photon fields, the density of which significantly exceeds the density of magnetic field, the effect of transition of Compton cooling from the Thomson regime to Klein-Nishina regime plays important role in formation of electron spectra and related with them energy spectra of synchrotron and inverse Compton radiation components. A possible example of such a source is the binary pulsar PSR B1259-63/SS2883 [1]. In this system a millisecond pulsar is orbiting around the massive Be2 star with tempreture $T \simeq 2.3 \cdot 10^4$ K and luminosity $L_{\text{star}} \simeq 3.3 \cdot 10^{37}$ erg/s. This implies huge photon densities, especially at epochs of the pulsar passage near the periastron, when the density of photons achieves $w_{\text{ph}} = L_{\text{star}}/4\pi R^2 c \simeq 1 \cdot (R/10^{13} \text{ cm})^{-2} \text{ erg/cm}^3$. Thus, for the magnetic field $B \simeq 1$ G (the corresponding energy destity $B^2/8\pi \simeq 0.5 \text{ erg/cm}^3$), which is estimated from the MHD treatment of the termination of the pulsar wind [2, 3], the energy density of photon field exceeds the energy density of magnetic field. This means that while for electrons of relatively low energy the energy losses are dominated by inverse Compton scattering, for TeV electrons the losses are dominated by synchrotron radiation (because of the suppressed Compton cross-section due to the Klein-Nishina effect). Although the cooling time in both energy regimes behaves as $t_{\text{cooling}} \propto 1/E_e$, the absolute scales differ by a factor of 3. On the other hand in the transition rigion (from 10 GeV to 1 TeV) the cooling time essentially deviate from the dependence $1/E_e$. This leads to the formation of unusual spectra of electrons and the related electromagnetic radiation. Obviously this effect is very important for interpretation of synchrotron X-rays and IC γ -rays. Such radiation componets were predicted from the unique binary pulsar

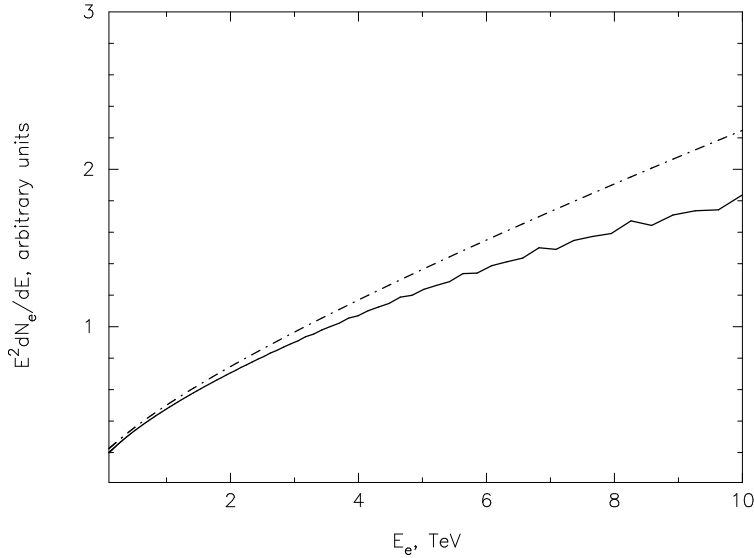


FIGURE 1. The steady state energy distribution function of electrons obtained within the continuous loss approximation (dashed line) and from the exact solution of the Boltzmann equation (solid line). The temperature of blackbody radiation is assumed $T = 2.3 \cdot 10^4$. The differential injection spectrum of electrons is taken as $q(E_e) \propto E_e^{-2}$. The results are shown in arbitrary units. Note that the ignorance of the Klein-Nishina effect would give much steeper steady state distribution $E_e^2 dN/dE \propto E_e^{-1}$

PSR B1259-63/SS2883 [2, 4, 5]. A similar scenario can be realized in the microquasar LS 5039 although in this case the TeV electrons have a different origin – most likely they are accelerated in the continuous jet originating from the compact star [6].

Bellow we investigate the importance of several effects for calculations of the electron distribution and corresponding synchrotron and IC energy spectra in binary systems with powerful optical star. These are, in particular, the approach of the continuous energy loss approximation for electrons, the Klein-Nishina effect and the anisotropy in distribution of the target radiation field.

THE ELECTRON DISTRIBUTION FUNCTION

To be specific, here we consider a systems similar to PSR B1259-63/SS2883 (for details see [1, 2]). We performed the analysis of the system assuming a power-law injection spectrum for electrons with exponential cut-off formed at the termination shock [7]. The energy distribution of electrons is determined by radiative losses; the impact of adiabatic losses we discuss elsewhere.

Although the continuous energy loss approximation is often used for determination of the electron distributions in ambient radiation field, this approximation *a priori* does not guarantee adequate accuracies, especially in the Klein-Nishina regime where the interactions have catastrophic character. The applicability of this approach we inspected comparing the results with ones obtained from the solution of the Boltzmann equation which appropriately treats the catastrophic energy losses (see Fig.1). In order to demonstrate the difference of the results, we assumed that the magnetic field $B = 0$.

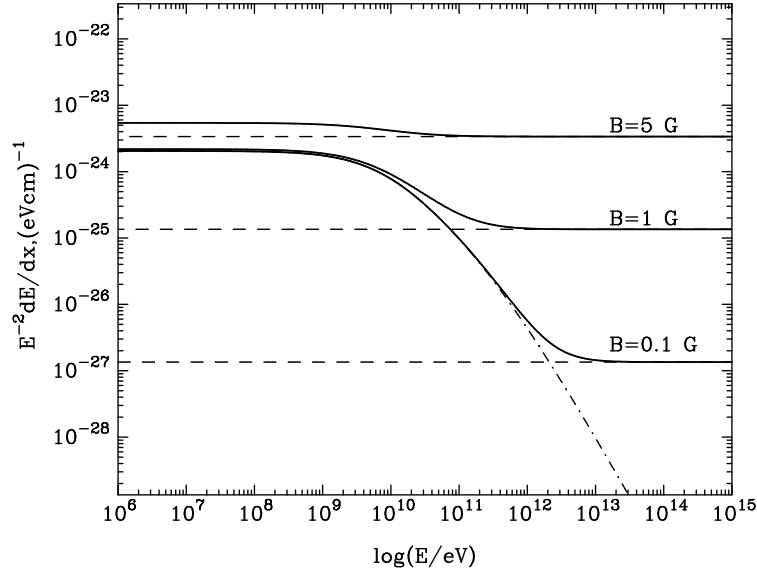


FIGURE 2. Energy lose rates of electrons. The dashed lines correspond to the synchrotron losses, the dot-dashed lines to IC losses, and the solid lines to the total radiative losses.

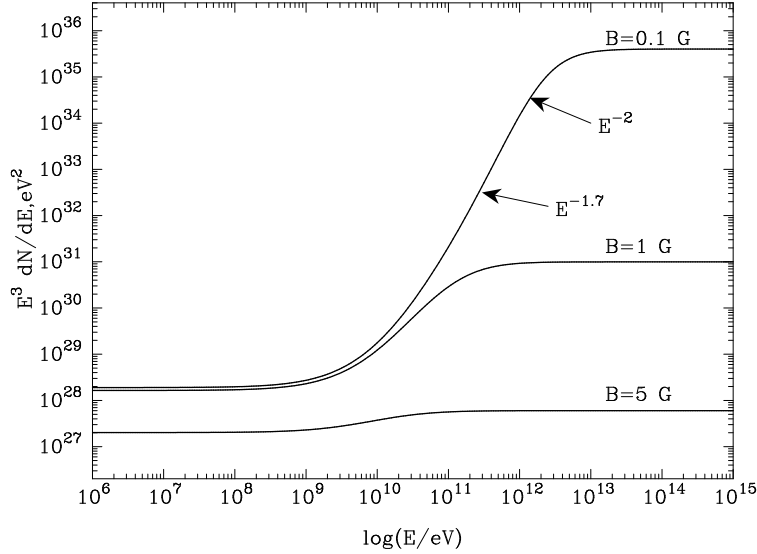


FIGURE 3. The electron steady state energy distribution functions for three different magnetic fields. The electron injection spectrum is assumed in the form $E_e^{-2} e^{-E_e/E_{\text{cut}}}$ with $E_{\text{cut}} \rightarrow \infty$.

One can see that, despite the fact that the scattering proceeds in the deep Klein-Nishina regime (the parameter $b = 4(3kT)E_e/(mc^2)^2 \simeq 90(E_e/\text{TeV}) \gg 1$), the continuous lose approximation describes the electron distribution within an accuracy less than 20% for $E_e \leq 10 \text{ TeV}$. Since this energy range is relevant for the production of synchrotron X-rays and TeV γ -rays, in what follows we present results obtained within much simpler continuous energy lose approximation.

Within this approach the steady state distribution of electron has the following form

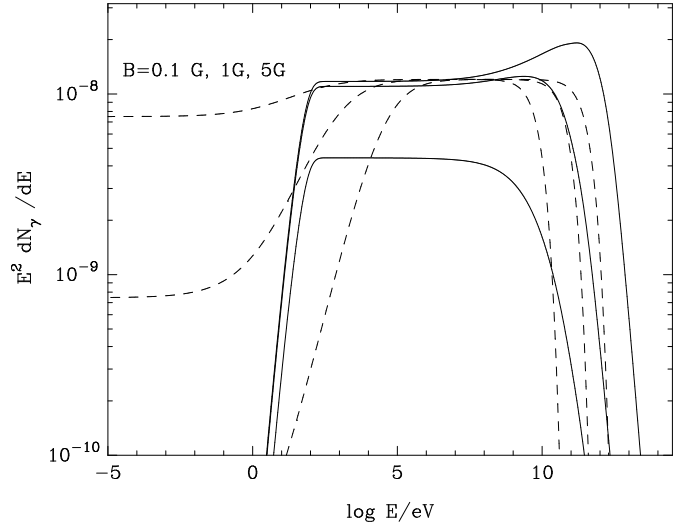


FIGURE 4. Spectral energy distributions of synchrotron radiation (dashed lines) and IC γ -rays (solid lines) calculated for the steady state electron distributions shown in Fig.3

$N_e(E_e) = \frac{1}{|\dot{E}_e|} \int_{E_e}^{\infty} q(E_e) dE_e$: here $q(E_e)$ is injection rate and \dot{E}_e is energy lose rate. The synchrotron and IC losses in the Thomson regime have the same energy dependence $\dot{E}_e \propto E_e^2$; in this case the ratio of synchrotron and IC losses equals to the ratio of the energy densities in the magnetic and photon fields. In the Klein-Nishina regime the Compton lose rate is almost energy independent $\dot{E}_{ic} \propto const$. Thus, in the radiation dominated environments energy lose rate may have very specific energy dependence.

This is demonstrated in Fig.2 for a fixed value of the photon energy density $w = 1 \text{ erg/cm}^3$ and temperature $T = 2.3 \cdot 10^4 \text{ K}$, but for three different values of the ambient magnetic field, $B = 0.1 \text{ G}$, 1 G , and 5 G . Correspondingly, the steady state spectra of electrons significantly depend on the strength of the magnetic field. While the synchrotron and Thomson losses make the electron spectrum steeper, the losses in the Klein-Nishina regime at the presence of a low magnetic field lead to the hardening of the electron spectrum. In the case when the magnetic field density is comparable or less than the target photon density, one should expect quite irregular electron spectra, especially in the transition region (see Fig.3). The electron spectra shown in this figure are calculated for a pure power-law injection spectrum, $q(E_e) \propto E_e^{-2}$, for three different magnetic fields. In the case of losses dominated by synchrotron radiation and/or by Thomson scattering, the steady state spectrum of electrons is $dN/dE \propto E_e^{-3}$. On the other hand, at the absence of magnetic field the steady state electron spectrum formed in the deep Klein-Nishina regime is very hard, close to $dN/dE \propto E_e^{-1}$. However, since for the assumed magnetic fields and the energy density of the star light, the broad band spectra of electrons have more complicated forms as shown in Fig.3. In low energy region we see indeed E_e^{-3} type spectrum with significant hardening in the transition region from 10 GeV to 1 TeV. Note that at very high energies the Compton losses are suppressed and the synchrotron losses dominate; therefore the electron spectrum again obtains a E_e^{-3} form. However, in reality the spectrum at such high energies depends strongly on the high-energy cutoff in the injection spectrum. This is demonstrated in Fig.5 (top panel), where the injection

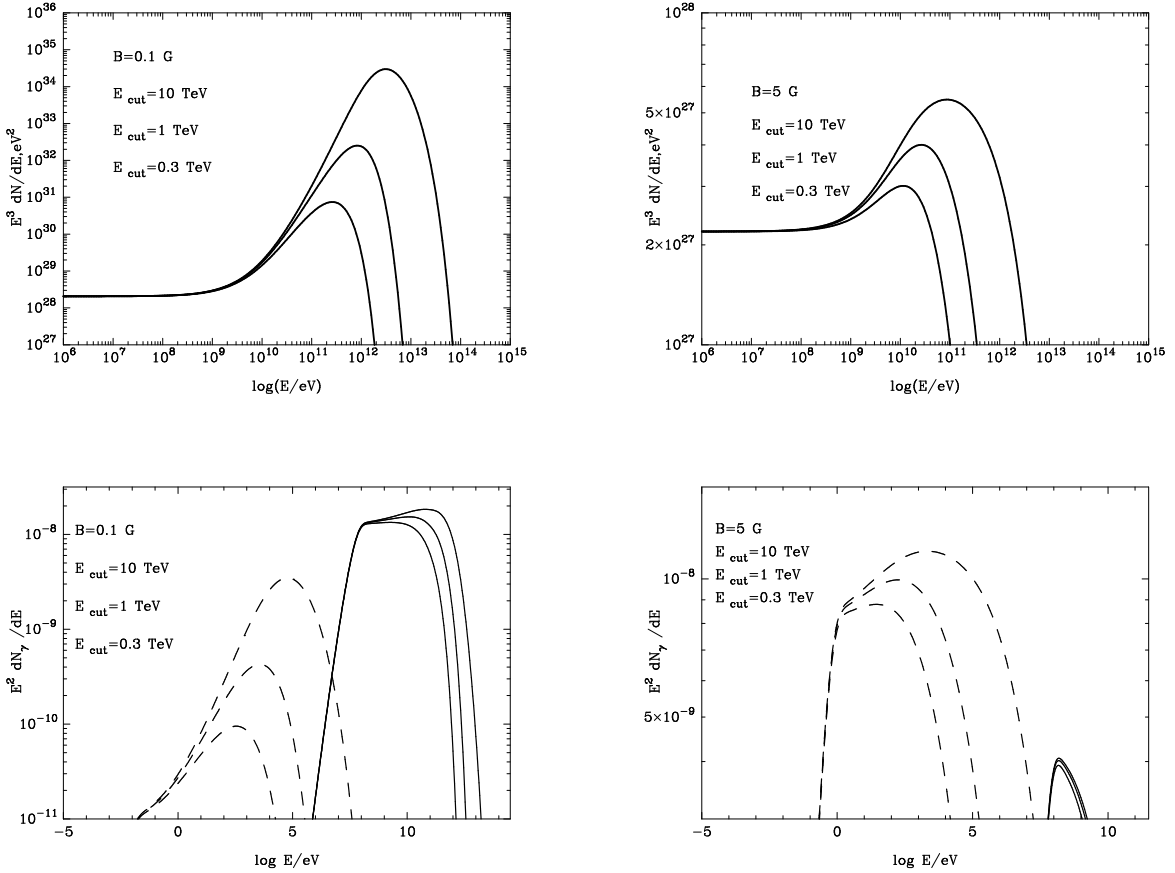


FIGURE 5. Top panel: The same as in Fig.3 but for fixed magnetic fields, $B = 0.1\text{G}$ (left panel) and $B = 5\text{G}$ (right panel) and for three different cutoff energies, $E_{\text{cut}} = 0.3 \text{ TeV}$, 1 TeV and 10 TeV . Bottom panel: Spectral energy distributions of synchrotron (dashed lines) and IC (solid lines) radiation components calculated for the steady state electron distributions shown in the top panel.

spectrum is given in the form $q(E_e) = E_e^{-2} e^{-E_e/E_{\text{cut}}}$, with three different cutoff energies, $E_{\text{cut}} = 0.3, 1$, and 10 TeV .

SPECTRAL ENERGY DISTRIBUTION OF RADIATION

The spectra of synchrotron and IC radiation components corresponding to the electron distributions in Fig.3 are shown in Fig.4. Note that in this figure the synchrotron spectra extend to very high energies, which is the result of the assumption of absence of the high energy cutoff in the injection spectrum of electrons. On the other hand the IC spectrum extends to very low energies because of absence of a low-energy cutoff in the injection spectrum of electrons. In Fig.5 we present more realistic spectra assuming both low- and high-energy cutoffs in the electron injection spectrum. In this case the synchrotron and IC components are well separated in the spectral energy distribution of radiation.

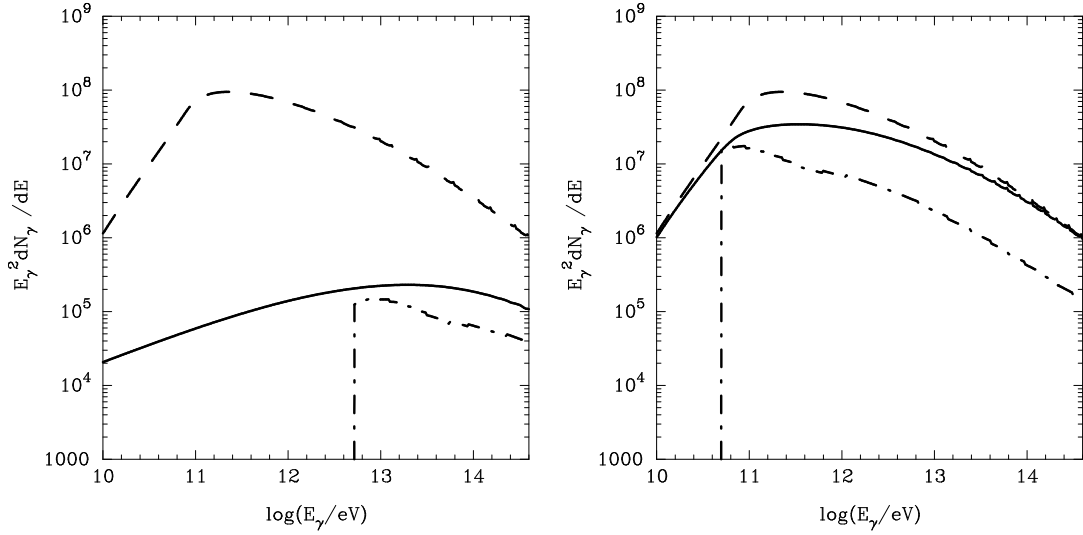


FIGURE 6. Spectral energy distribution of the IC radiation for a truncated power-law electron spectrum, E_e^{-2} ($100\text{GeV} \leq E_e \leq 10^3\text{TeV}$), calculated using the accurate cross-section (solid lines), the cross-section average over the angle (dashed lines) and δ -function approximation of the cross-section (dot-dashed lines), calculated for two different interaction angles, $\theta = 5^\circ$ (left panel) and $\theta = 45^\circ$ (right panel).

THE IMPACT OF THE ANISOTROPY OF THE TARGET PHOTON FIELD

Since in the binary system the relativistic electrons "see", for any given time, the radiation from the star at certain angles, it is important to use the precise double differential cross-section, $d\sigma/d\Omega dE$, for calculations of both the spectral and temporal characteristics of radiation. This is demonstrated in Fig.6 where the spectral energy distribution of the IC radiation is shown for different interaction angles using (i) the accurate cross-section, (ii) cross-section average over the angle, and (iii) δ -functional approximation like the one used in Ref. [4]. The results show that both the average cross-section and δ -functional approximation fail to describe appropriately the broad band energy spectrum, as well as absolute γ -ray fluxes.

REFERENCES

1. Johnston, S., et al., *MNRAS*, **279**, 1026–1036 (1996).
2. Tavani, M., and Arons, J., *ApJ*, **477**, 439–463 (1997).
3. Ball, L., Melatos, A., Johnston, S., and Skjæraasen, O., *ApJ*, **514**, L39–L42 (1999).
4. Kirk, J., Ball, L., and Skjæraasen, O., *Astroparticule Physic*, **10**, 31–45 (1999).
5. Murata, K., Tamaki, H., Maki, H., and Shibasaki, N., *AdSpR*, **33**, 601–604 (2004).
6. Bosch-Ramon, V., and Paredes, J. M., *A&A*, **417**, 1075–1081 (2004).
7. Kennel, C., and Coroniti, F., *ApJ*, **283**, 694–709 (1984).